Travelling waves in biology: Lecture 3

1 Intracellular calcium waves

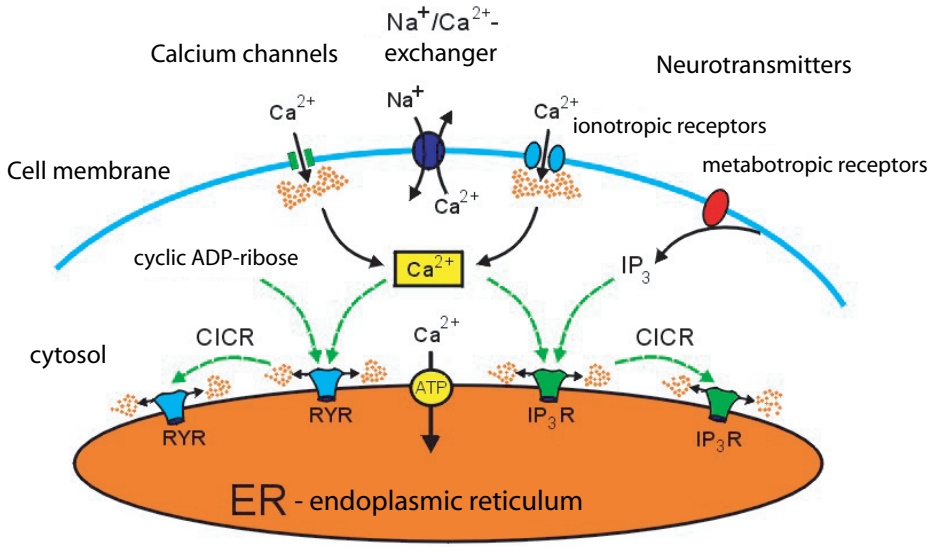

The fire-diffuse-fire (FDF) model [1] is relevant to the study of travelling wave behaviour observed when Ca^{2+} is released from internal stores in living cells. Ca^{2+} is stored intracellularly in the endoplasmic or sarcoplasmic reticulum at 2–3 orders of magnitude greater than its concentration in the cytosol and is released by a nonlinear feedback process referred to as calcium-induced calcium release (CICR). CICR involves Ca^{2+} release through Ca^{2+} channels that are receptors for IP_3 (inositol (1,4,5)-trisphosphate). These channels are activated at slightly elevated levels of cytosolic Ca^{2+} and then inactivated as the level of Ca^{2+} rises further. This mechanism for generating oscillations in the concentration of cytosolic free Ca^{2+} is believed to underlie the waves that propagate as intra and intercellular waves over distance as large as 1mm with speeds of between

5 and 20 μms^{-1} . When coupled to the kinetics of Ca^{2+} reuptake into stores (by Ca^{2+} ATPases), the CICR mechanism can lead to excitability and oscillations. Initiation sites or *hot spots* have been found to spontaneously release Ca^{2+} and can trigger a wave that spreads via the CICR process. Burst-like wave behaviour is commonly seen in immature Xenopus oocytes and in cardiac myocytes where saltatory waves propagate with a non-constant shape. Importantly, long ranged Ca^{2+} waves are capable of synchronising the activities of different cytoplasmic regions of a single cell, such as cortical granule exocytosis after egg fertilisation. In contrast to a saltatory wave, these waves have a continuous nature. Both types of wave are thought to be supported by the same mechanism, namely CICR. The existence of such long range spatial and temporal signalling by Ca^{2+} is one of the most significant findings of the last decade in the field of intracellular signalling and has stimulated many experiments for the elucidation of the role of Ca^{2+} waves in cell regulation. A major success of the FDF model is the natural description of both saltatory and continuous travelling waves.

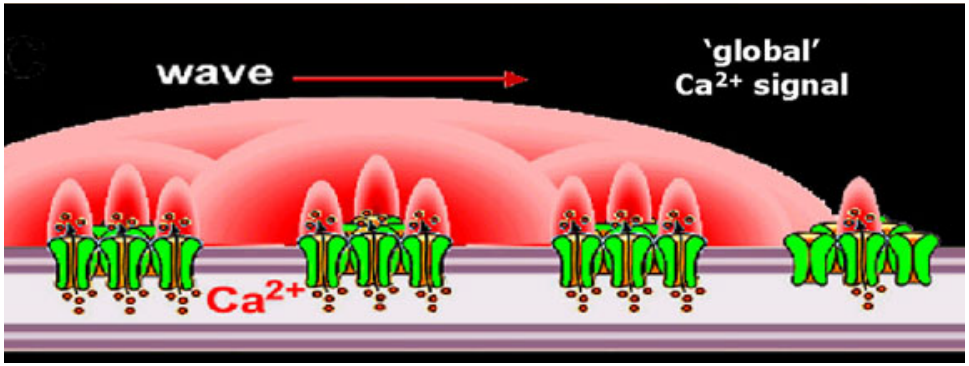

The FDF model incorporates descriptions of the two major fluxes between the endoplasmic reticulum and the cytosol. The first is due to a pump which drives the Ca^{2+} up the gradient from the cytosol back into the endoplasmic reticulum and the second arises when the IP_3 receptor/calcium channel opens and causes a large flux from the endoplasmic reticulum into the cytosol. After an open channel closes via inactivation, it cannot reopen for some time during which it is in a *refractory* state. Thus the release of Ca^{2+} by intracellular stores is self-regulating. Such events are commonly referred to as Ca^{2+} *puffs* or *sparks* and are the elementary events underlying Ca^{2+} waves. The FDF model provides a caricature of Ca^{2+} release events that allows one to study an array of Ca^{2+} release sites that can interact via diffusion of Ca^{2+} and the triggering of a CICR like mechanism.

For further discussion see [2, 3].

2 The fire-diffuse-fire model - breaking translation invariance

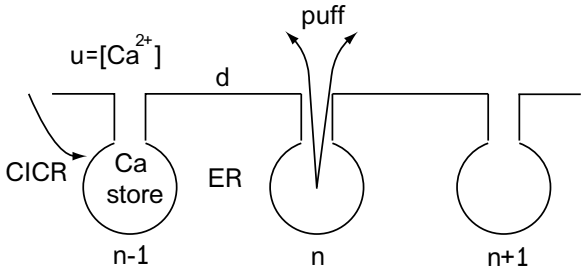

The one dimensional FDF model consists of a regular array of point-source release sites with lattice spacing d, embedded in a continuum in which calcium ions diffuse. Denoting the concentration of Ca^{2+} ions by $u(x,t)$ the FDF model is given by the following partial differential equation

$$\frac{\partial u}{\partial t} = -\frac{u}{\tau_d} + D\frac{\partial^2 u}{\partial x^2} + \sum_{n=-\infty}^{\infty} \delta(x - x_n)\eta(t - T^n), \quad x \in \mathbb{R}, t > 0. \tag{1}$$

Note that $x_n = nd$ is the location of the nth Ca^{2+} release site and the first time that $u(x_n,t)$ crosses a threshold u_c from below is denoted by T^n. Hence, the FDF model assumes that the site at x_n releases only one Ca^{2+} puff at a time, T^n, determined by

$$T^n = \inf\{\ t \mid u(x_n,t) > u_c,\ \frac{\partial u(x_n,t)}{\partial t} > 0\}.$$

The function $\eta(t)$ describes the shape of the Ca^{2+} puff and is considered as a rectangular pulse-shape given by

$$\eta(t) = \frac{\sigma}{\tau_R}\Theta(t)\Theta(\tau_R - t)$$

where $\Theta(x)$ is a step function ($\Theta(x) = 0$ for $x < 0$, $\Theta(x) = 1$ for $x \geq 0$), σ is the strength of the calcium puff and τ_R is the duration of Ca^{2+} release. The inclusion of the decay time τ_d in (1) models the time-scale associated with the action of the pumps that resequester the Ca^{2+} back into the stores. Under normal physiological conditions pumps that are embedded in the membrane consume nucleotide trisphosphates and pump the Ca^{2+} up the gradient from the cytosol back into the stores. In the absence of any sources ($\sigma = 0$) equation (1) is equivalent to the cable equation that is often used to model the spread of voltage in a passive unbranched dendritic cable.

3 Travelling waves

The FDF model is capable of composing global signals (travelling waves) from elementary events (puffs or spikes). The solution of (1) can be expressed in terms of the Green's function of the cable equation as

$$u(x,t) = \frac{\sigma}{\tau_R} \sum_{n=-\infty}^{\infty} \int_{T^n}^{T^n+\tau_R} dt' G(x - x_n, t - t')$$

where

$$G(x,t) = \frac{e^{-t/\tau_d}}{\sqrt{4\pi D t}} e^{-x^2/(4Dt)} \Theta(t)$$

We consider travelling waves which satisfy $T^n = n\Delta$ so that the speed of threshold crossing events is given by $c = d/\Delta$. Moreover, we restrict attention to the case where $\Delta > \tau_R$ so that only one site is releasing Ca^{2+} at any one time. The, as yet, undetermined parameter Δ will be referred to as the period of a wave as it measures the time between successive release events that make up a saltatory travelling pulse. Assuming that only the sites with index up to N have crossed threshold we have that

$$u(x,t) = \frac{\sigma}{\tau_R} \sum_{n=-\infty}^{N} \int_0^{\min(t-n\Delta,\tau_R)} dt' G(x - nd, t - t' - n\Delta), \quad t > t_N.$$

Since we are only interested in long time solutions that cause sites with increasing n to cross threshold we consider the large N limit and neglect all terms in the above sum with $n \leq 0$. Hence,

$$u(Nd, N\Delta) = \frac{\sigma}{\tau_R} \sum_{n=0}^{N-1} \int_0^{\tau_R} dt' G((N-n)d, (N-n)\Delta - t'). \tag{2}$$

Introducing

$$H(x,t) = \frac{1}{\tau_R} \int_0^{\tau_R} G(x, t - t') dt',$$

gives

$$u(Nd, N\Delta) = \sigma \sum_{n=1}^{N} H(nd, n\Delta).$$

Note that $\lim_{\tau_R \to 0} H(x,t) = G(x,t)$. Hence, one may determine the speed of the travelling wave in a self-consistent manner by demanding

$$\lim_{N\to\infty} u(Nd, N\Delta) = u_c.$$

This is an implicit equation for $\Delta = \Delta(u_c)$, and hence $c = c(u_c)$.

Note from (2) that waves do not propagate with an invariant shape even though the threshold crossing times occur on a regularly spaced temporal lattice. A saltatory travelling wave solution to the FDF model is illustrated in figure 1. Note the large increase in the concentration of Ca^{2+} ions just after a release event. The saltatory nature of the wave may be directly attributed to the fact that release sites are not spread continuously throughout the system. Continuum models that neglect the discreteness of release sites are more appropriate for the study of travelling waves with constant profiles.

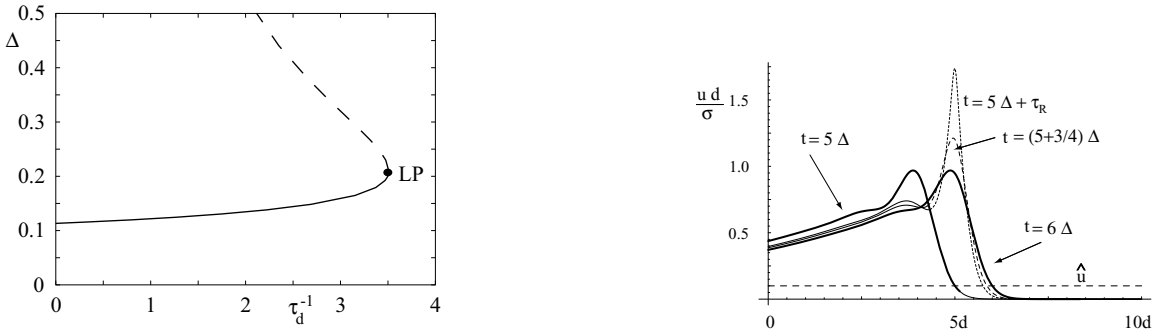

Figure 1: An example of a stable saltatory travelling wave analytically determined by equation (2) with $N = 5$. The period Δ of the wave is determined self-consistently as $\Delta = 0.17$ for the choice of parameters $t_d = 1$, $\tau_D = d^2/D = 1$, $\tau_R = 0.1$ and $\widehat{u} = u_c d/\sigma = 0.1$

Stochastic FDF

Add noise to the threshold: $u_c \to u_c + \text{noise}$, to mimic the stochastic nature of calcium release [4].

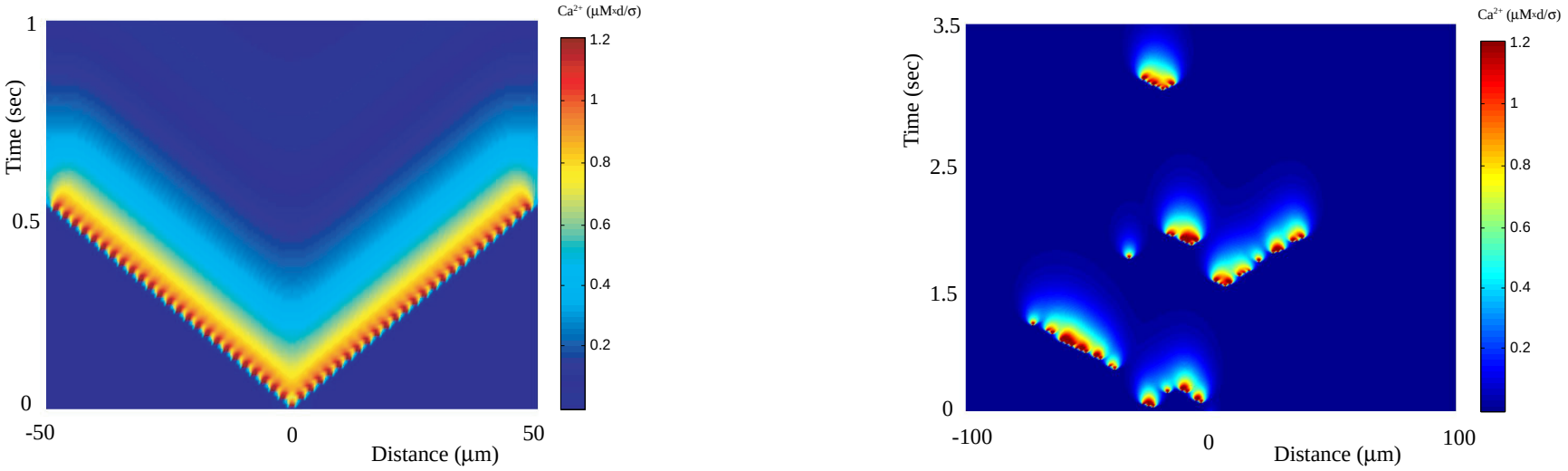

Figure 2: Left: An example of two lurching pulses moving out from the center of a deterministic one dimensional FDF model with 50 regularly spaced release sites and free boundary conditions. Right: Stochastic FDF model - much more like biological reality!

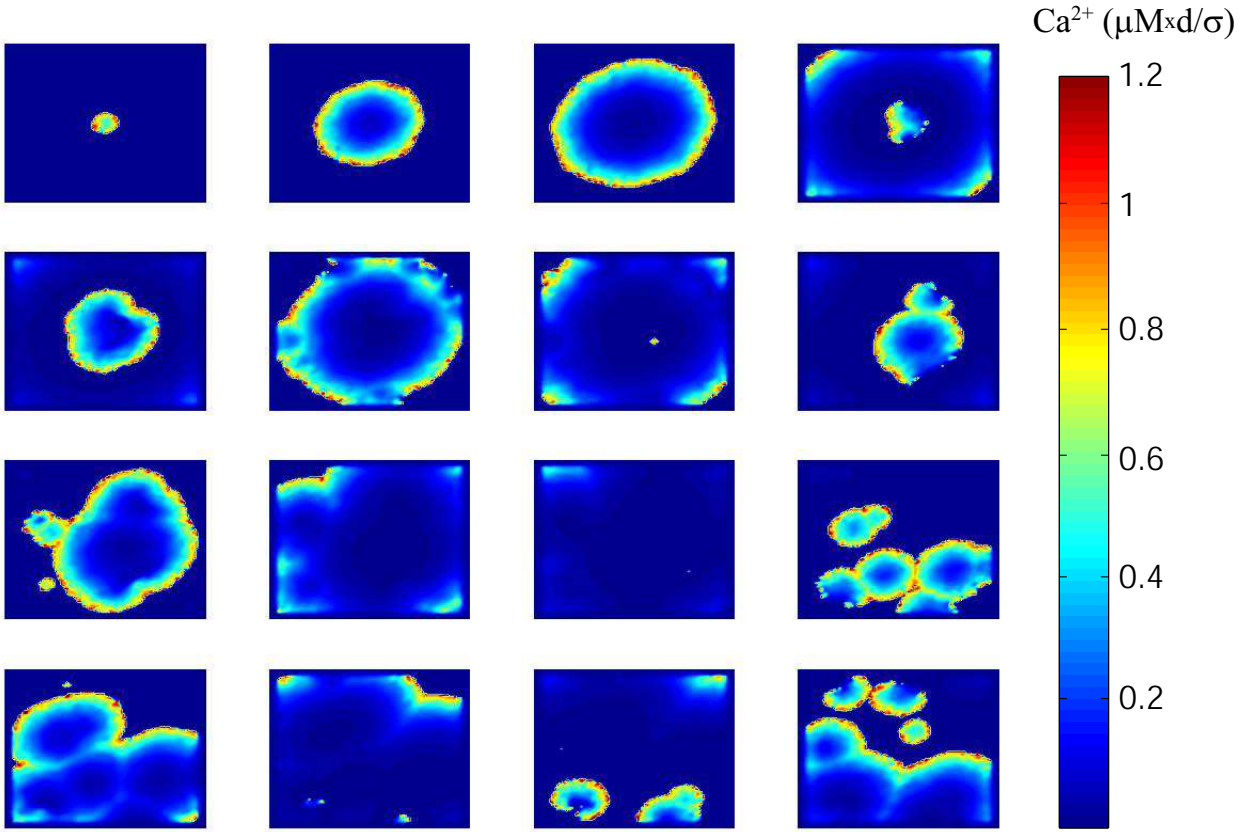

Figure 3: Temporal sequence snapshots for the two-dimensional stochastic FDF model with low noise. Frames are presented every 0.45s starting in the top left corner and moving rightward and down. An initial seed in the center of the cell model leads to the formation and propagation of a circular front. Spiral waves form in the wake of the wave by spontaneous nucleation. These can be destroyed in wave-wave collisions and created by spontaneous nucleation.

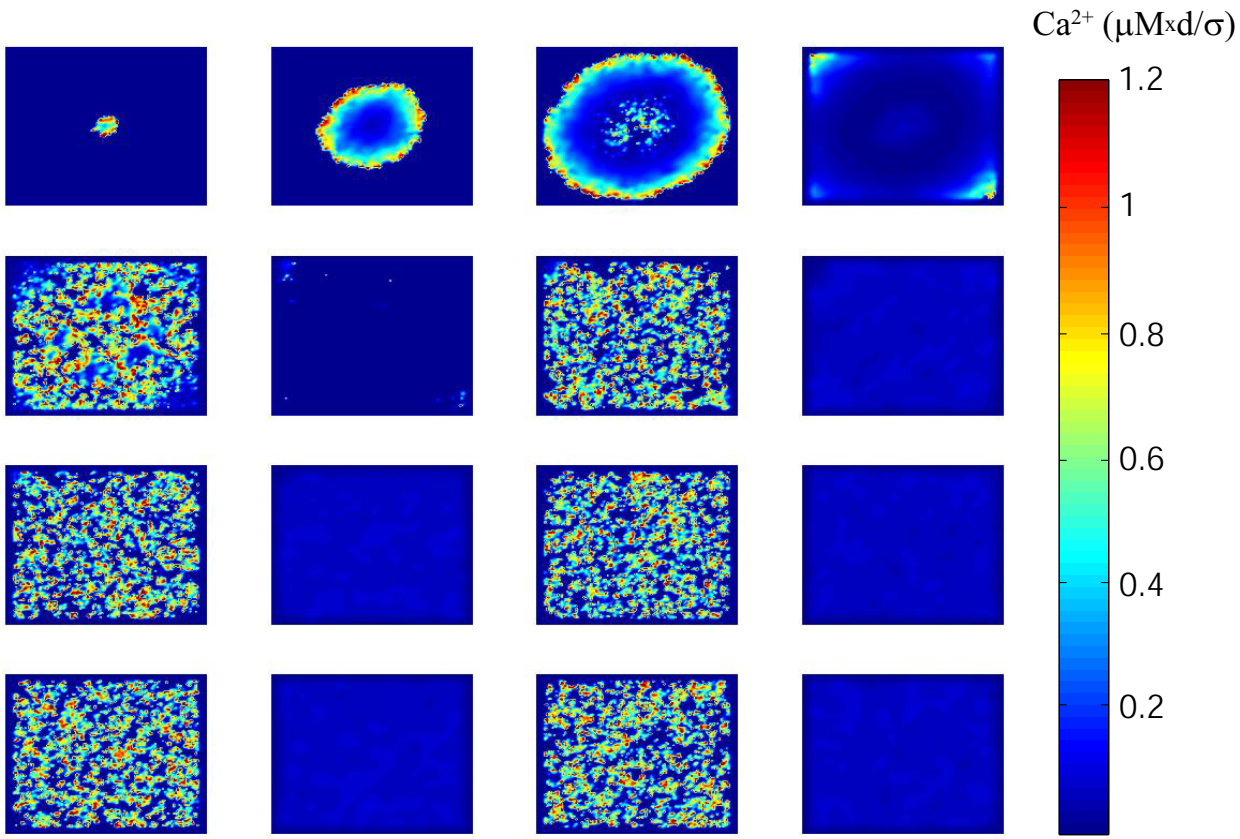

Figure 4: Temporal sequence snapshots for the two-dimensional stochastic FDF model with high noise. Frames are presented every 0.45s starting in the top left corner and moving rightward and down. An initial seed leads to the formation of a circular travelling front. In the wake of the wave there is periodic and near simultaneous release from a large number of stores, typical of systems exhibiting array enhanced coherence resonance.

4 A continuum calcium bi-domain model

Here we explicitly model the fact that the Ca^{2+} content in the intra-cellular Ca^{2+} store is in fact finite and should be more properly described with a bidomain model as in [5]. Introducing the ratio between the effective volumes of the ER store and the cytosol as γ, the bidomain model takes the form

$$\frac{\partial c}{\partial t} = J_{rel} - J_{pump} + D\frac{\partial^2 c}{\partial x^2},$$
$$\frac{\partial c_{er}}{\partial t} = -\gamma^{-1}[J_{rel} - J_{pump}] + D_{er}\frac{\partial^2 c_{er}}{\partial x^2}.$$

Here

$$J_{rel}(x,t) = (c_{er}(x,t) - c(x,t)) \sum_m \eta(t - T^m(x)).$$

The release times $T^m(x)$ are determined by a threshold process such that

$$T^m(x) = \inf\{t \mid c(x,t) \geq c_{th},\ t > T^{m-1}(x) + \tau_R\},$$

and τ_R is an absolute refractory time-scale.

In the bidomain model the calcium pump flux must account for the Ca^{2+} on both sides of the ER membrane. Here we consider the linear pump model

$$J_{pump} = \frac{c}{\tau} - \frac{c_{er}}{\tau_{er}}.$$

4.1 The shunt model

Take c_{er} constant and set $\tau_{er}^{-1} = 0$. Consider a single release event, $T(x) = x/\nu$. Introducing $\xi = \nu t - x$ we may re-write the original equations of motion (for a solitary travelling release event) in the co-moving frame as $c = c(\xi, t)$, where c satisfies

$$\left(\frac{\partial}{\partial t} + \nu\frac{\partial}{\partial \xi}\right) c = -\frac{c}{\tau} + D\frac{\partial^2 c}{\partial \xi^2} + \eta(\xi/\nu)(c_{er} - c).$$

A stationary profile $c(\xi, t) = c(\xi)$ in the co-moving frame satisfies the ODE

$$(d_\xi - m_+(\xi))(d_\xi - m_-(\xi))c = F(\xi), \qquad F(\xi) = -\frac{c_{er}}{D}\eta(\xi/v),$$

where

$$m_\pm(\xi) = \frac{v \pm \sqrt{v^2 + 4\epsilon(\xi)D^2}}{2D}, \qquad \epsilon(\xi) = \frac{1}{D}\left(\frac{1}{\tau} + \eta(\xi/v)\right).$$

Introducing $z = (d_\xi - m_-(\xi))c$, we see that

$$z(\xi) = G_+(\xi, 0)\left[z(0) + H(\xi)\int_0^\xi G_+(0, \xi')F(\xi')d\xi'\right],$$

where

$$G_\pm(\xi, \xi') = \exp\left(\int_{\xi'}^{\xi} ds m_\pm(s)\right).$$

For $z(\xi)$ to be bounded as $\xi \to \infty$ we require

$$z(0) = -\int_0^\infty G_+(0, \xi')F(\xi')d\xi'.$$

The corresponding solution for $c(\xi)$ is given by

$$c(\xi) = G_-(\xi, 0)\left[c_{th} + \int_0^\xi G_-(0, \xi')z(\xi')d\xi'\right].$$

For $c(\xi)$ to be bounded as $\xi \to -\infty$ we require

$$c_{th} = z(0)\int_{-\infty}^0 G_-(0, \xi')G_+(\xi', 0)d\xi'.$$

Note that for $\xi < 0$ $m_\pm(\xi) = k_\pm$, where

$$k_\pm = \frac{v \pm \sqrt{v^2 + 4D/\tau}}{2D}.$$

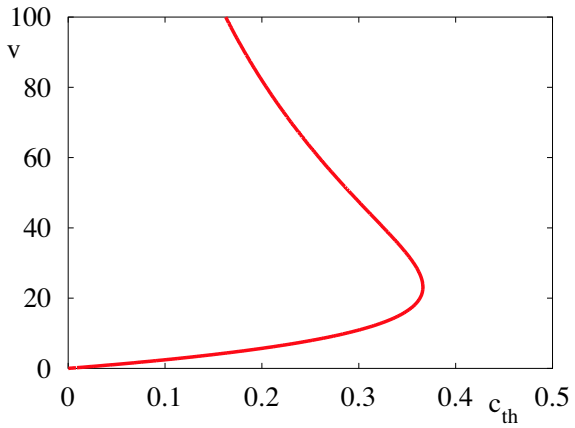

Figure 5: Speed of a solitary wave as given by (3) with $\eta(\xi) = \overline{\eta}\Theta(\xi)\Theta(\Delta - \xi)$. $\nu = \nu(c_{th})$, with $D = 30$, $c_{er} = 100$, $\Delta = 0.05$, $\tau = 0.01$ and $\overline{\eta} = 1$. Of the two branches of solutions, the slower is always unstable.

Hence, we have the elegant result that the speed of the wave is determined by the equation

$$c_{th} = \frac{z(0)}{k_+ - k_-},$$

As an example consider $\eta(\xi) = \overline{\eta}\Theta(\xi)\Theta(\Delta - \xi)$. In this case $z(0)$ is easily calculated as

$$z(0) = \frac{\overline{\eta} c_{er}}{D} \frac{1 - e^{-m_+ \nu \Delta}}{m_+}, \qquad m_+ = \frac{\nu + \sqrt{\nu^2 + 4(\tau^{-1} + \overline{\eta})D}}{2D}. \tag{3}$$

For sufficiently small c_{th}/c_{er} there are a pair of solutions to (3), as illustrated in Fig. 5.

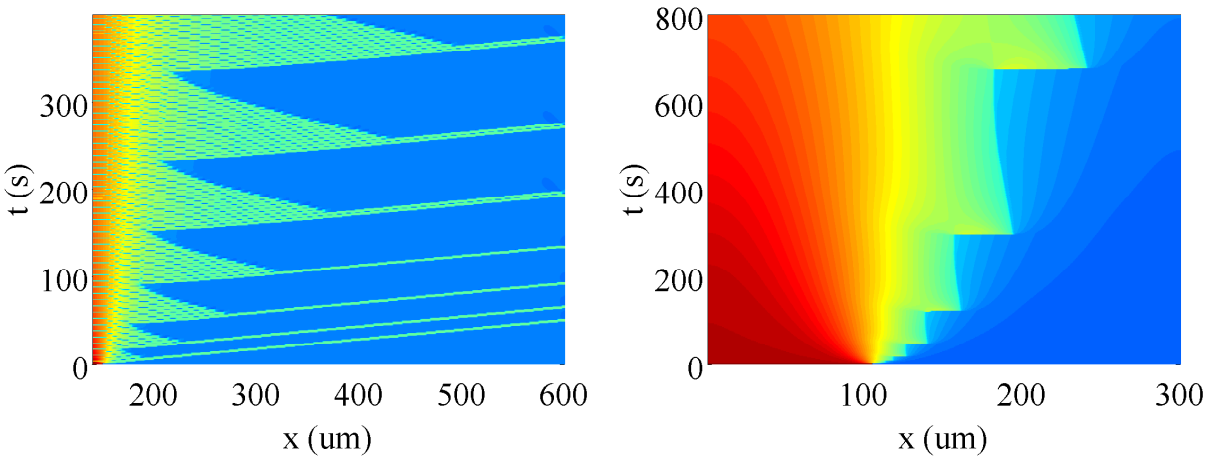

Figure 6: Tango waves in the vicinity of the point of dynamic instability.

4.2 Tango waves in the full bi-domain model

Travelling fronts and pulses can be constructed in a similar manner for the full bi-domain model. In this case a linear stability analysis shows that the faster branch of solutions can undergo a dynamic instability (not possible for the pure shunt model). Some numerical examples of waves beyond a dynamic instability point are shown in figures 6 and 7. In contrast to pulse and front solutions that travel with a constant speed in one direction, we observe waves that propagate in a back-and-forth manner. Such a dynamical phenomenon was first reported in [5] and named as tango waves. The left panel in figure 6 resembles earlier findings, especially with respect to the wave form and to the emergence of additional pulses. Whenever a tango wave reverses its direction after invading the low calcium concentration region, pulses are set off, which travel to the right with constant speed. The number of pulses can increase in the course of time. The first four tango waves initiate only one pulse, whereas proceeding ones give rise to two pulses. The form of the tango wave changes appreciably when we alter γ as can be inferred from the right panel in figure 6. Instead of fingering tango waves, the wave front is now more compact and the amplitude of the back-and-forth movement is much smaller.

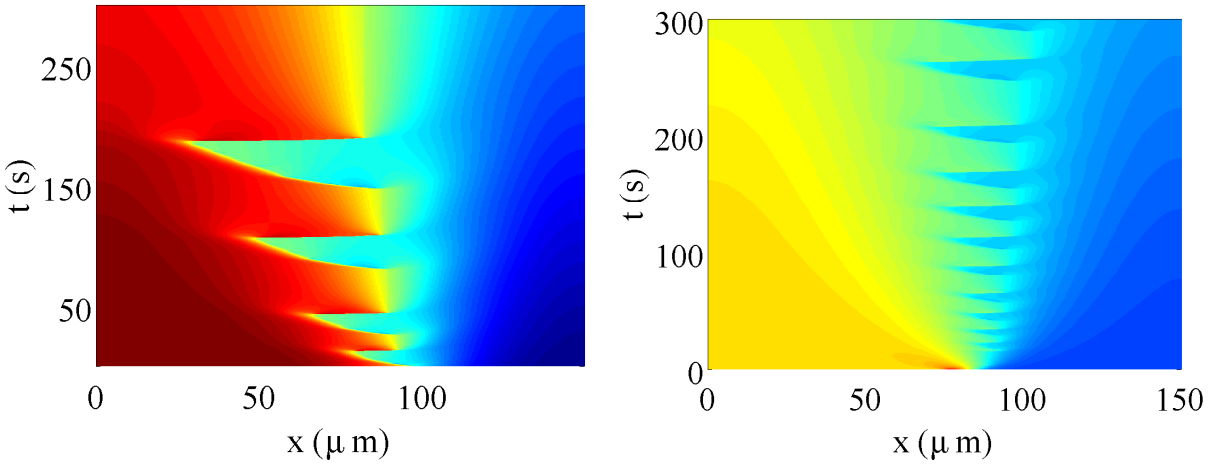

Figure 7: Reversed tango waves for two different initial calcium concentration profiles.

Figure 7 illustrates that tango waves possess a larger variety of forms than already suggested by figure 6. Here, the front extends from a state of low calcium concentration to the one of high calcium concentration. Although going into the reverse direction, the shape of the moving edge is similar to the one in figure 6. A comparison between the two panels in figure 7 with respect to the interface between the high and the low calcium concentration state reveals that it moves to the left in the left panel, but to the right in the right panel. Therefore, the state of low calcium concentration will eventually occupy the whole space in the former example, whereas the same is true for the state of elevated calcium concentration in the latter case.

References

[1] J E Keizer, G D Smith, S Ponce Dawson, and J Pearson. Saltatory propagation of Ca^{2+} waves by Ca^{2+} sparks. *Biophysical Journal*, 75:595–600, 1998.

[2] S Coombes. The effect of ion pumps on the speed of travelling waves in the fire-diffuse-fire model of Ca^{2+}. *Bulletin of Mathematical Biology*, 63:1–20, 2001.

[3] S Coombes, R Hinch, and Y Timofeeva. Receptors, sparks and waves in a fire-diffuse-fire framework for calcium release. *Progress in Biophysics and Molecular Biology*, 85:197–216, 2004.

[4] S Coombes and Y Timofeeva. Sparks and waves in a stochastic fire-diffuse-fire model of calcium release. *Physical Review E*, 68:021915, 2003.

[5] Y-X Li. Tango waves in a bidomain model of fertilization calcium waves. *Physica D*, 186:27–49, 2003.